Team 5 Final Report for 16.100

Javier Chico, Kristine Bridges, Matthew McGillick

December 5, 2021

Contents

1 Introduction

In this document, we introduce a revolutionary passenger aircraft complete with a fully-electric power source, vertical takeoff and landing (VTOL) capabilities, and a solar array that spans the upper surface area of the plane. In particular, this report analyzes our aircraft's weight, range, stability, aerodynamics, and numerous other vital qualities using a variety of techniques, ranging from low-level estimates to high-quality computational fluid dynamics (CFD) models.

In the interest of providing a more complete picture of the iterative design process, the report features two primary divisions: the preliminary/draft section and the final section. The preliminary section, Section 4, focuses on the initial estimates and calculations made as a proof-of-concept; the final section analyzes the calculations and data created to improve the draft design, yielding our final aircraft model.

The supplemental Jupyter Python notebook includes code detailing all calculations that appear in this document.

2 Objectives

1. Payload: 5 people + luggage
2. Range: over 1000 Km
3. Cruise Speed: 140 ms^{-1}
4. Solar cell arrangement on the wing + fuselage. Assume 40% efficiency.
5. Electricity storage in lithium ion batteries. We are assuming futuristic batteries with 650 Wh/Kg energy density [1] and between 2000 Kg and 3000 Kg of them. The batteries are modular so that they can be removed for shorter flights, added for longer flights, etc.
6. Osprey-style VTOL system with large propellers on the wingtips which can change between hover and cruise position. Additionally, there is a large propeller on the nose of the fuselage (i.e. Cessna style), allowing for a smoother transition between VTOL and cruise.
7. Aircraft dimensions (in meters):
   (a) Fuselage: For drag calculations a streamlined cylinder is assumed, of dimensions: 6 m long, 1 m radius
   (b) Wing: wingspan = 10 m, chord = 2.5 m.
   (c) Vertical tail: 1.8m tall, chord ranging from 0.96m at the root to 0.69m at the top.
   (d) Horizontal tail: wingspan = 5 m, chord = 0.7 m

[1] see `https://www.nasa.gov/sites/default/files/atoms/files/650_whkg_1400_whl_recharg_batt_new_era_elect_mobility_ymikhaylik_0.pdf`

8. Weight: estimated using the procedure described in class. Excluding batteries, we have an upper bound of 1500 Kg if made of aluminium (density 2.7 g/cc), if made with composite materials/carbon fibre of density 1.55 g/cc, the weight will be lower. Weight estimate is derived in the next section. The mass of the batteries is taken as 2000 Kg for the calculations, although variations of this parameter are also considered.

3 Weight Estimate

The weight of the fuselage was determined to be between 397-457 kg using two different assumptions. (We will take the larger value into account for the total aircraft weight.)

1. The shape of the fuselage is approximately cylindrical with a thickness of .004 m using a Boeing 747 as reference.

2. The weight of the fuselage is proportional to the number of passengers.

Using the E-350 Expedition aircraft as a reference, and the fact that the average weight of a person is 62kg (with an estimated 50kg of luggage each), the payload weight is estimated as 560 kg. The weight of the main wing (with NACA 4412 airfoil) and stabilizing wings is determined using the following equations:

$$\frac{W_{wing}}{g} = 0.7\frac{1}{0.12}AR^{3/2} * S_{ref}^{1/2}\frac{2700}{2.1 \cdot 10^8}(W_{fuse} + W_{pay})$$

$$W_{tail} = 0.2 \cdot W_{wing}$$

This gives us a total wing weight of around 36kg. Using the X-57 Maxwell as reference, we will have 3 large high-lift motors and propellers at around 25kg each. Overall, this gives us a total aircraft weight of 1128kg which we can estimate as 1500kg to account for the landing gear, electrical engines, control systems, air conditioning, etc.

4 Preliminary/Draft Altitude, power and Energy calculations.

4.1 Determination of optimal cruise altitude

To determine the optimal cruise altitude atmospheric data was obtained from the EngineeringToolbox[2]. We can try to get an analytical solution for the optimal density and work backwards to find the optimal altitude. We know the induced drag will be (up to a $\mathcal{O}(1)$ factor)

$$D_i = \frac{2L^2}{\pi b^2 V_\infty^2 \rho} = \frac{K}{\rho}$$

and the skin friction drag will have to contributions, from the wings and the fuselage:

$$D_f = \frac{1}{2}\rho V_\infty^2 (S_w C_{dw} + S_f C_{df}) = \Gamma\rho$$

Hence the total drag on the plane when it is cruising will be

$$D = \frac{K}{\rho} + \Gamma\rho$$

We are interested in the optimal (least drag) altitude for the plane. The only variable that varies wrt to altitude is air density, so this question is equivalent to finding the optimal air density and then seeing at

[2] https://www.engineeringtoolbox.com/air-altitude-density-volume-d_195.html

what altitude that value of the density is present. Taking a derivative of the drag wrt ρ, and finding the value for which the derivative is zero, ρ^*

$$-\frac{K}{\rho^2} + \Gamma = 0 \Longrightarrow \rho^* = \sqrt{\frac{K}{\Gamma}}$$

This means

$$\rho^* = \sqrt{\frac{2L^2}{\pi b^2 V_\infty^2} \frac{2}{V_\infty^2 (S_w C_{dw} + S_f C_{df})}}$$

Furthermore we can substitute this into the drag equation to find the drag at the optimal altitude:

$$D^* = \frac{K}{\sqrt{\frac{K}{\Gamma}}} + \Gamma \sqrt{\frac{K}{\Gamma}} = \sqrt{K\Gamma} = \frac{2L\sqrt{C_f S_f + C_w S_w}}{\sqrt{\pi} b}$$

The following values are assumed for the draft calculations:

1. $C_{dw} = 0.005$
2. $C_{df} = 0.05$ as we picture the fuselage as a streamlined body, but not incredibly streamlined.
3. $S_w = bc$, where b is the wingspan (10 m) and c is the chord (2.5 m).
4. $S_f = 2\pi r_f l_f$, with the fuselage approximated as a cylinder, with $r_f = 1$ m, $l_f = 6$ m.
5. $L = g \cdot (1500 + \text{Battery Weight})$ for now. We take a lower value of gravity, $g = 9.7$ as in cruise condition we fly really high, so g is slightly smaller compared to the value observed on the surface of the Earth.

Using this numerical values, we obtain $\rho^* = 0.1379 Kg$ m-3. We can also check this graphically 2:

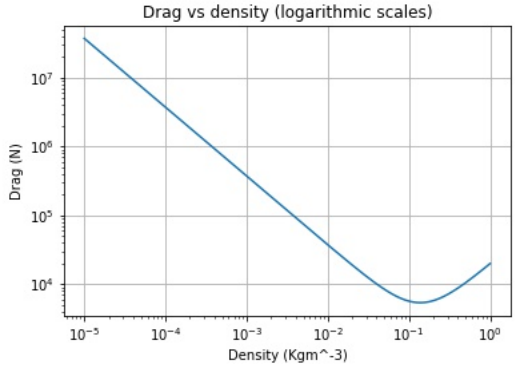

Figure 1: Drag as a function of air density (draft)

Hence interpolating from the following Figure 2, the optimal flying altitude is around 14 km a bit too high.

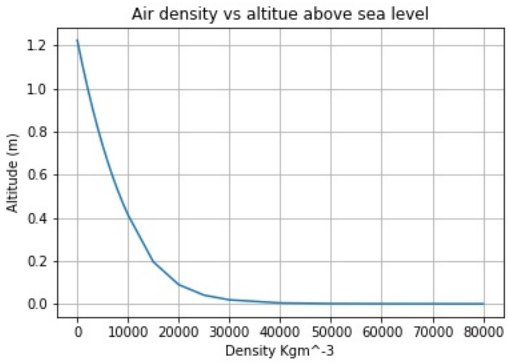

Figure 2: Air density as a function of altitude above sea level

The total drag at this optimal altitude is 5431 N.

We can also get a drag vs altitude graph combining both of the previous plots, in Figure 3. Note this plot is approximate as there are not many data points for the density-altitude function.

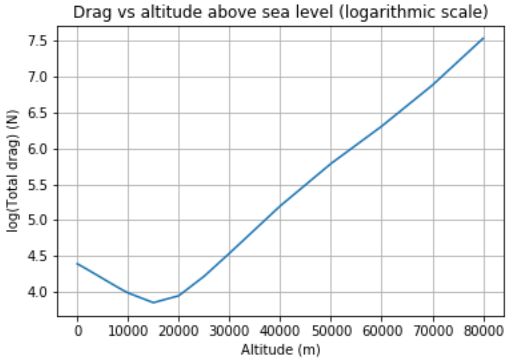

Figure 3: Drag as a function of altitude above sea level (draft)

4.2 Power Considerations

4.2.1 Power required for VTOL

From Quiz 1, we are given an equation for the "Figure of Merit," or FoM, of a VTOL aircraft. Using this formula, we see a relation between the FoM, power, thrust, and the rotor area of an aircraft, giving power as

$$P = \frac{T^{3/2}}{FoM\sqrt{2\rho A}}$$

For a numerical approximation of VTOL power, the below values are assumed as:

1. $FoM = 0.75$
2. $T = L$ for L as defined in Section 3
3. $\rho = 1.225$ Kg m^{-3}
4. $A = 2 \cdot \pi \cdot (\frac{d}{2})^2$ for $d =$ diameter of the VTOL propellers in meters, with $d = 7$ m

Using these values, the approximated required VTOL power is 990500 W, or 991 kW.

4.2.2 Power required for cruise

We can get the power required for cruise as the total drag times the cruise speed. Using the formula from the previous section for the drag at optimal air density, we see that

$$P = DV_\infty = \frac{2L\sqrt{C_f S_f + C_w S_w}}{\sqrt{\pi} b} V_\infty$$

Hence the total power required for cruise flight is 760350 W, or 760 kW. This translates to roughly 1020 CV. (Horsepower)

4.2.3 Electric motors

There will be three different options for electric motors, depending on the needs of the customer, and chosen by them:

- **WEG** An affordable, powerful, with a single W50 motor[3]. This motors provide 1000 HP (750 KW) and are rated at 96% efficiency. (Preferred option, allows the plane to climb quickly to cruise altitude)
- **Wright Motors** A more powerful, heavier, and far more expensive option with two 2MW Wright Technologies Motors[4], still in development. This engine configuration would allow for considerably higher cruise speed, but it would drain the batteries at a faster rate.
- **H3X**: a less powerful, but lighter and more power dense option, using a two engine configuration for each propeller. These motors produce 250KW, but only weigh 15 Kg[5], allowing the plane more maneuverability and range. Furthermore these engines have a rated efficiency of 96%.

4.3 Energy and Range

4.3.1 Short flight configuration

We can answer the energy question by noting that with 2000 Kg of batteries (short flight configuration), we have, in total, 1300 kWh; assuming the electric motors have an efficiency of 90% (which could be improved based on the estimates from the previous section, but we will assume 90% to account for other possible losses), this means that the available energy is 1170 kWh. To get the range, we note that the work done by the plane is

$$W = D \cdot x$$

where x denotes the distance travelled. Hence we can get an estimate for range given the battery weight. Converting into Joules and dividing by the drag, we get the range in meters, which turns out to be 775 Km.

4.3.2 Long flight configuration

We can repeat the previous calculation but with 3000 Kg of batteries, and the resulting range is 904 Km. Note, however, that as the mass of the plane is different, to get this number a different density has been used, etc.

[3] https://www.weg.net/catalog/weg/VC/en/Electric-Motors/Large-Induction-Motors/TEFC-Motors/W50-Line/W50-1000-HP-4P-7006-07-3Ph-4160-V-60-Hz-IC411---TEFC---Foot-mounted/p/13038062

[4] https://www.weflywright.com/technology#motors

[5] https://www.h3x.tech/

4.4 Solar effects

This aircraft is meant to be flown in regions with reliably sunny weather, such as the Tropics, the Middle East, Northern Africa, or Australia. The average annual solar radiation at the top of the Earth's atmosphere is 1361 W/m^2; at sea level it is closer to 1100 W/m^2, so a lower bound at the plane's cruising altitude is approximately 1200 W/m^2 on a sunny day. Hence, assuming a 40% efficiency (with slight assumptions made with advancements in photovoltaic technology) in the solar panels mounted on the upper body of the aircraft, the total solar power produced by the plane is 23976 W, or 23.9 kW. This means we will be able to produce around 3.1534% of the required power from solar cells in the short flight configuration!

How will this affect the range? We can recompute the range taking into account solar effects for the short flight configuration, which gives us 800.78 Km, so around 25 Km for free.

4.5 Theoretical Maximum range (no solar effects, excluding lift considerations)

It is clear that increasing the battery weight will increase the range, but there's a critical battery weight which provides the maximum range; from there, any increase in battery weight will not offset the increased induced drag, hence decreasing the range. We will find that value in this section.

By letting η be the energy density times the motor efficiency, B the battery mass and m_d the mass of the plane excluding the batteries. Hence the lift force required is

$$L = g(m_d + B)$$

and the total available energy is ηB. Moreover, we can write the drag components

$$D_i = \frac{2(g(m_d + B))^2}{\pi b^2 V_\infty^2 \rho} = \alpha(m_d + B)^2$$

$$D_f = \frac{1}{2}\rho V_\infty^2 (S_w C_{dw} + S_f C_{df}) = \beta$$

$$D = \alpha(m_d + B)^2 + \beta$$

Hence the range, R, is the energy divided by the drag; in other words

$$R = \frac{\eta B}{\alpha(m_d + B)^2 + \beta}$$

We would like to maximize R with respect to B, so we can take a partial derivative and solve for B^*. However mathematically, it is easier to minimize $1/R$, as

$$\frac{1}{R} = \frac{\alpha(m_d + B)^2 + \beta}{\eta B} = \frac{1}{\eta}\left(\frac{\alpha m_d^2 + \beta}{B} + 2m_d\alpha + \alpha B\right)$$

Taking a derivative and setting equal to zero:

$$-\frac{\alpha m_d^2 + \beta}{B^2} + \alpha = 0$$

Taking the positive solution,

$$B^* = \sqrt{\frac{\alpha m_d^2 + \beta}{\alpha}} = \sqrt{m_d^2 + \frac{\beta}{\alpha}}$$

Substituting back into the equations:

$$B^* = \sqrt{m_d^2 + \frac{1}{2}\rho V_\infty^2 (S_w C_{dw} + S_f C_{df}) \frac{\pi b^2 V_\infty^2 \rho}{2g^2}}$$

With our parameters this would be 11237 Kg of batteries, giving a theoretical maximum range of 3298 Km when flying at the altitude previously specified. However, at this weight the coefficient of lift required is fairly high - 4.01 - so it is not feasible. It does provide us with an idea of how the range of the plane behaves as we vary the battery mass. In Figure 4 the relationship between range and battery mass is seen.

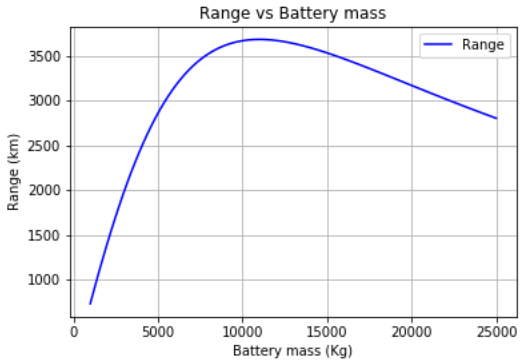

Figure 4: Variation of range with respect to battery mass (draft)

Although it would be interesting to optimize the range with respect to density and battery mass simultaneously, the resulting system of equations from setting the partial derivatives equal to zero has no physically meaningful solutions: it has no real, positive solutions for (ρ^*, B^*), so we must settle for optimizing one variable at a time.

5 Model design

5.1 3D model of the aircraft

The final model of our aircraft, created using Engineering SketchPad (ESP), is seen below, in Figure 5a and Figure 5b:

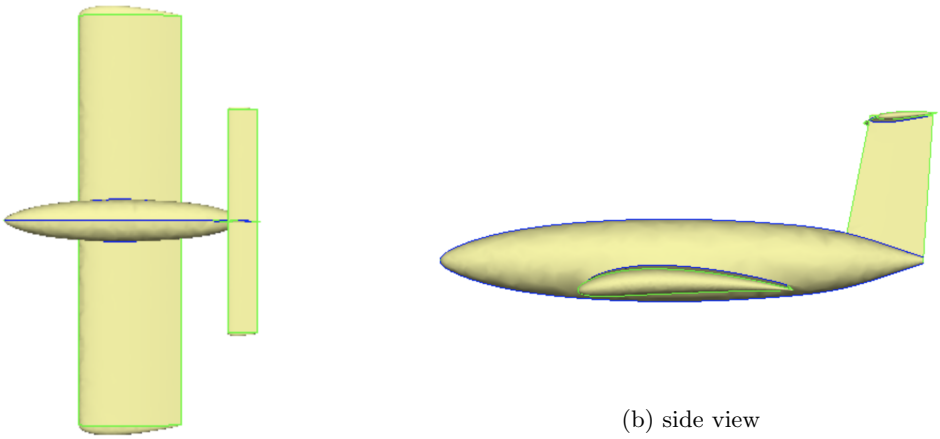

(a) top view

(b) side view

We can highlight several changes. Firstly, the fuselage has been modified so that it is more streamlined. This decreases drag and improves performance. Moreover, the horizontal tail has been shifted to the top of the vertical stabilizer, exposing it to the freestream. Finally, the horizontal stabilizer's angle of attack, α_H, was altered, to -4 degrees relative to the main wing.

5.2 Airfoil Selection for the main wing and the horizontal tail

The main wing will use the NACA 4412 airfoil. We choose this airfoil for several reasons:

1. The cruise speed is below Mach 0.8, so the effect of wave drag is irrelevant: therefore, the effect of camber on drag is not important. We are additionally interested in a high lift airfoil.

2. It provides a very high Lift-to-Drag ratio at low speeds, allowing us to transition to normal (i.e. non-VTOL) flight earlier in the journey. Moreover, it is very resistant to flow separation, with the flow starting to separate from the Trailing edge at around 9-10 degrees AoA, and maximum lift happens at around 18 degrees.

3. Furthermore, we can see from Figure 7 that the maximum L/D ratio is 175, very high. According to xfoil, this ratio is achieved at an angle of attack of 5 degrees. This is, of course, unrealistic for a full 3D aircraft.

The horizontal tail will use the NACA 0012 airfoil in order to address stability concerns, discussed further in Section 9.

5.2.1 Airfoil Performance

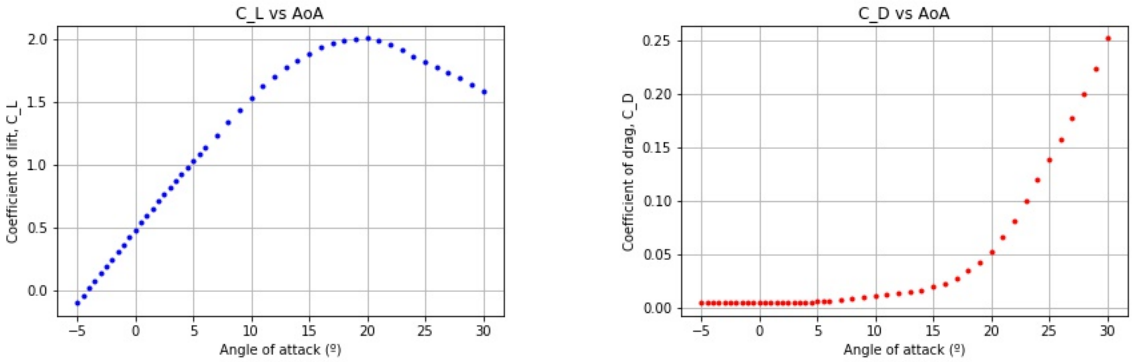

(a) Coefficient of lift

(b) Coefficient of drag

Figure 6: Airfoil Performance

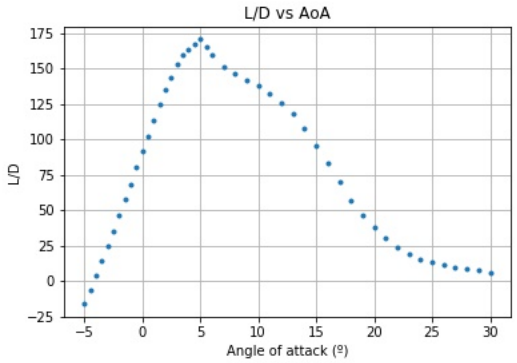

Figure 7: Lift vs Drag ratio for NACA 4412

It is interesting to study in further detail the airfoil at optimal L/D ratio, in Figure 8a and when flow separation is severe, in Figure 8b.

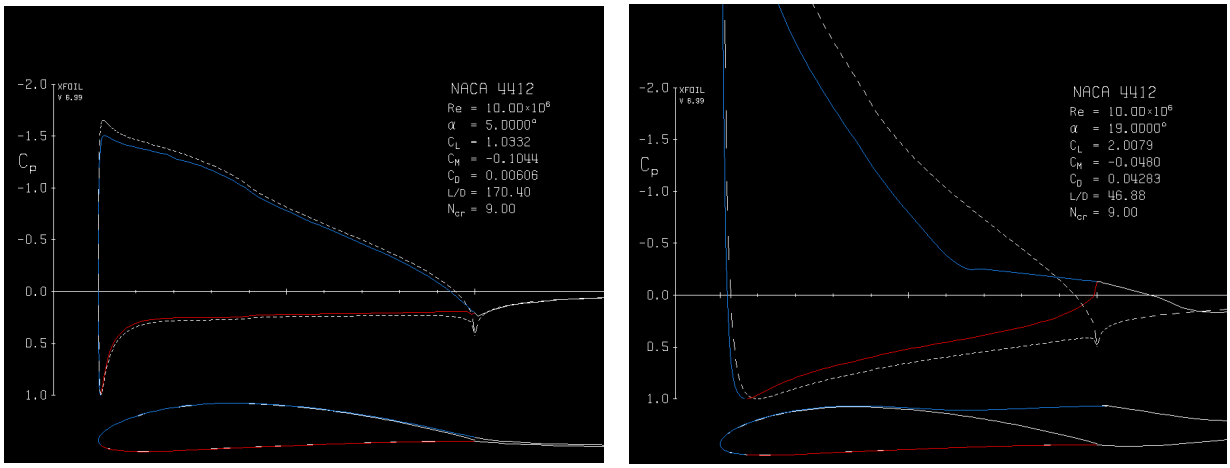

(a) Optimal LD ratio

(b) Severe flow separation

Figure 8: Airfoil characteristics at relevant angle of attacks

In Figure 8b we can confirm that the flow separates from the trailing edge, and it does so gradually. Even at this extreme angle of attack the airfoil is still generating significant lift.

5.3 Airfoil Selection for the Vertical Tail

For the vertical tail we opted to use a thin and symmetrical airfoil profile, in particular NACA 0004. Symmetry is required so that the plane is not biased, and it must be thin to have a minimal drag contribution.

5.4 Airfoil Selection for the Horizontal tail

For the horizontal tail, we selected a NACA 0012. The horizontal tail is positioned at a relative angle of attack of -4 degrees with respect to the main wing. We have opted to use a thick, symmetrical airfoil to increase the downwards lift, making the aircraft more stable.

5.5 Airfoil Selection for the Wing Propellers

We decided to use a propeller airfoil similar to the tiltrotor system present on the CV-22 Osprey. The below table compiles data found in a NASA paper by Ethan Romander: it details the varying airfoil of a prototype tiltroter aircraft's propeller.[6]

Table 1: Propeller Airfoil Design

r/R	**Airfoil**	**Thickness**
0.06	XN28	25.0%
0.50	XN18	16.0%
0.75	XN12	10.5%
1.00	XN09	8.0%

Within the table, r/R represents a location r as a portion of the full rotor length R. Additionally, the Thickness metric describes the thickness of the rotor with respect to the chord length of the aircraft's wing.

[6] https://rotorcraft.arc.nasa.gov/Publications/files/Romander_AHSVLDC2006.pdf

5.6 Airfoil Selection for the Nose Propeller

The nose propeller, similar to the wing propellers, uses a blended airfoil design based loosely on the Pipistrel P-812-164-F3A Propeller.

6 Computational Results: Cruise phase

The software Flex Compute was used to perform computation fluid dynamics on the airplane. This software solves the Reynolds Averaged Navier-Stokes equations. The flow for several angles of attack was computed.

6.1 CFD at 0 degrees angle of attack

CL:	2.1509e-1	CD:	2.1332e-2		
CFx:	2.1332e-2	CFy:	-1.5056e-4	CFz:	2.1509e-1
CMx:	5.5859e-5	CMy:	-2.1027e-1	CMz:	-1.6189e-4

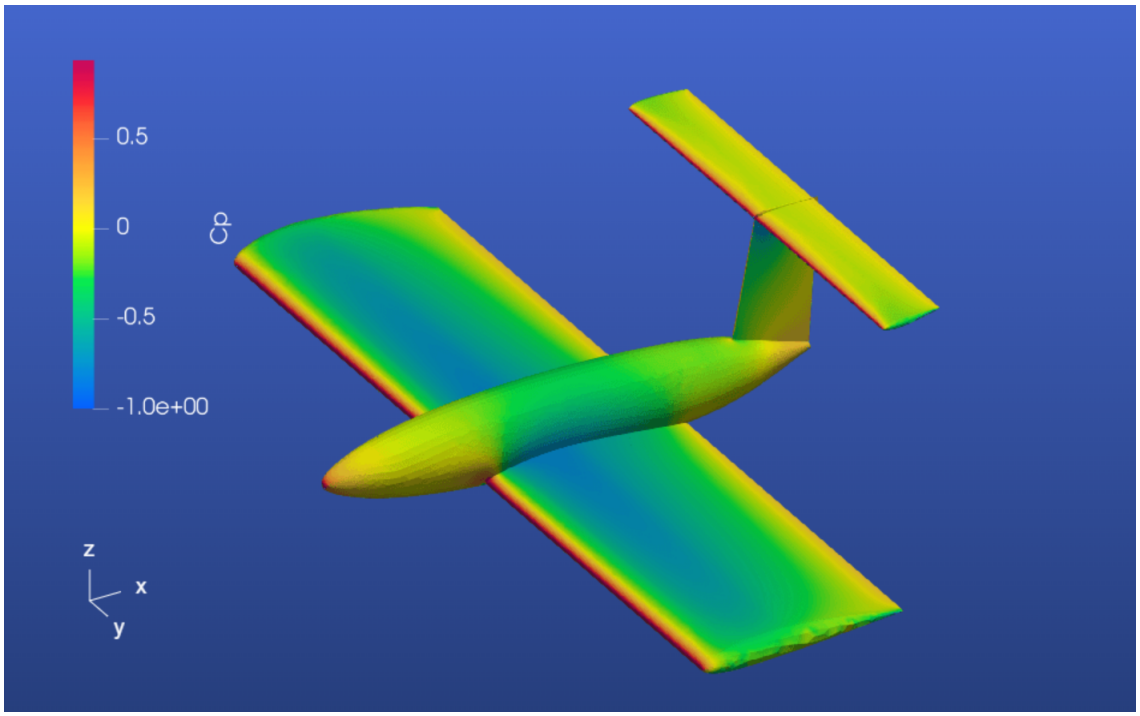

Figure 9: Pressure at 0 degrees AoA

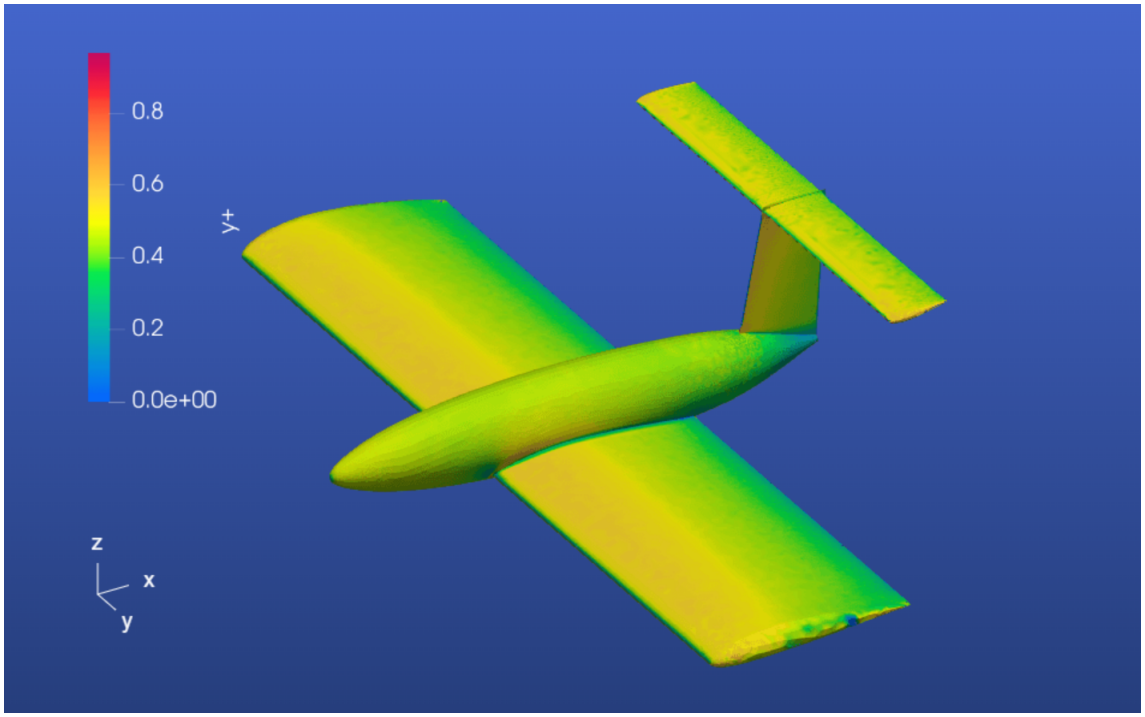

Figure 10: Check on CFD BL resolution

6.2 CFD at 4 degrees angle of attack

The following numerical values were obtained:

CL:	5.2360e-1	CD:	3.8965e-2		
CFx:	2.3455e-3	CFy:	-2.1167e-4	CFz:	5.2504e-1
CMx:	-7.6300e-5	CMy:	-5.2779e-1	CMz:	-2.1144e-4

We can see the coefficient of drag is around 0.04, close to the estimate used for the drag computation. Moreover, the coefficient of lift is also close to what we need. The lift-to-drag ratio is relatively high, around 13.438, meaning the aircraft cruises efficiently. In Figure 11 we can observe the pressure distribution, and Figure 12 checks the boundary layer (BL) is well resolved.

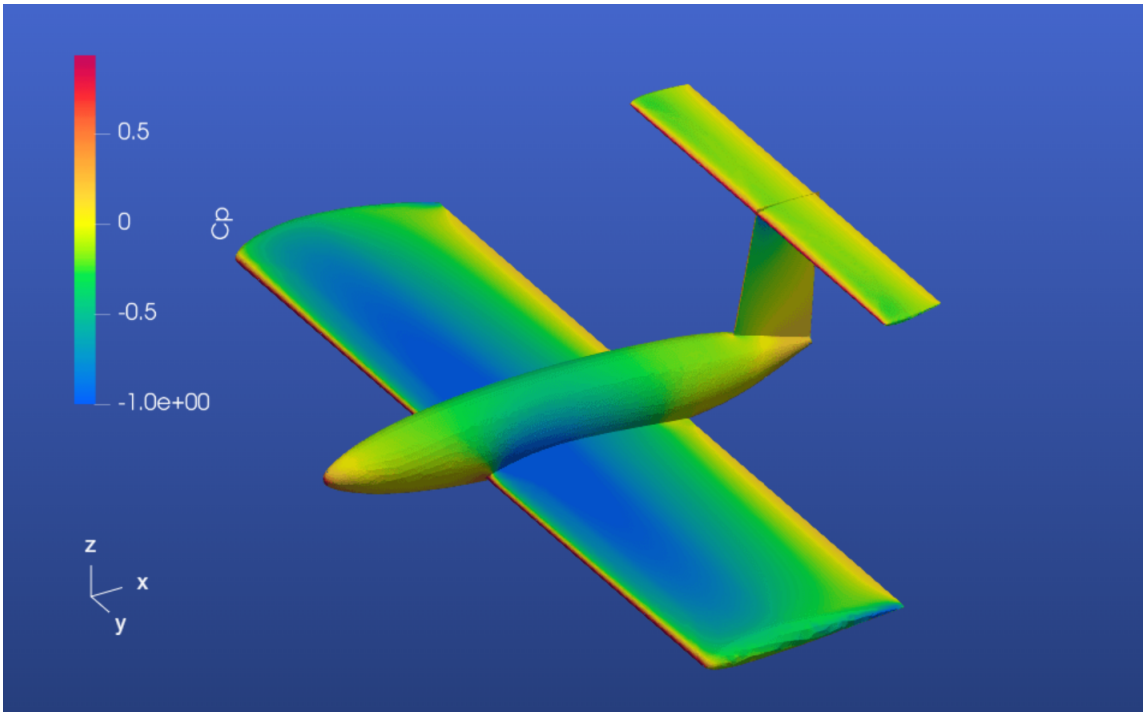

Figure 11: Pressure at 4 degrees AoA

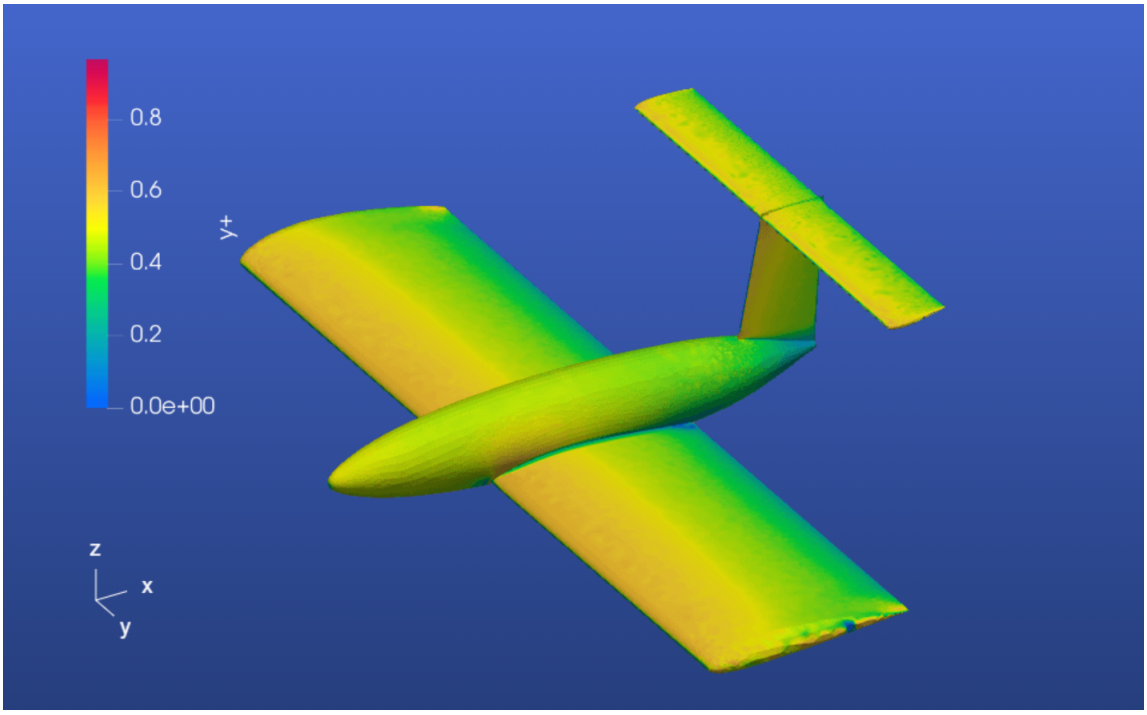

Figure 12: Check on CFD BL resolution

6.3 Wave Drag Check

In all of our calculations we assume Wave Drag is negligible. For this to be correct, we must ensure the flow stays subsonic around the aircraft. We can check this from the CFD, in particular checking if the maximum speed stays subsonic. We can see this in Figure 13.

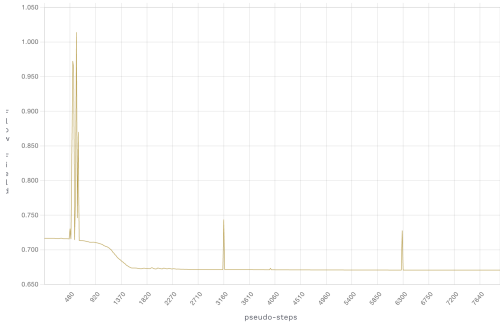

Figure 13: Maximum speed of the flow in cruise

Indeed, we confirm the flow stays subsonic around the aircraft (we are only interested in the value for the final iterations, when the CFD has converged), meaning our no wave drag assumption is correct.

7 Stability Analysis

7.1 Draft Report Stability Analysis

In our draft report, we observed that the center of lift of our aircraft became less negative (i.e. moved upstream) as the angle of attack increased. This meant that our draft aircraft was unstable: a small perturbation in the angle of attack, α, would result in a pitching moment that would amplify the change in α. Therefore, our draft aircraft would be unable to return to its original position when faced with disturbances during flight.

Using the results from the draft CFD, we constructed the following plots, in Figure 14. The angles of attack considered were 3,4, and 6. The center of lift is defined as:

$$C_{My}/C_L$$

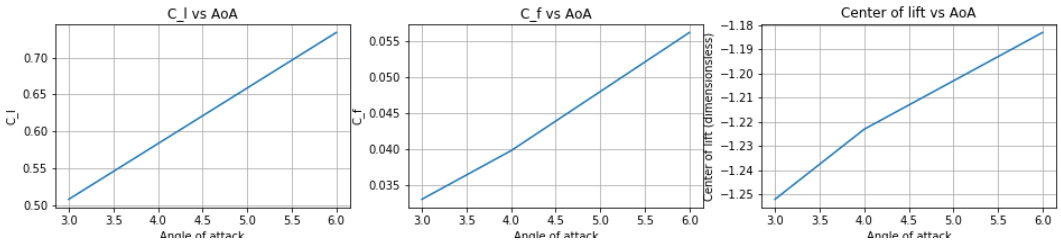

Figure 14: Results from the CFD

The above graphs clearly show that as α increases, the center of lift became less negative, moving further upstream.

7.2 Intermediate Stability Analysis

Following this analysis, we listed a number of possible solutions to this problem; the below list describes the solutions applied to our final aircraft.

1. Changing the airfoil of the horizontal tail to a thin, symmetric airfoil
2. Changing the angle of attack, α_h, of the horizontal tail in order to change the aerodynamic center of the aircraft
3. Changing the position/size of the horizontal tail

Applying the first and second items from the above list enabled us to construct the following plots, seen in Figure 15. The angles of attack are 3, 4, and 6, respectively.

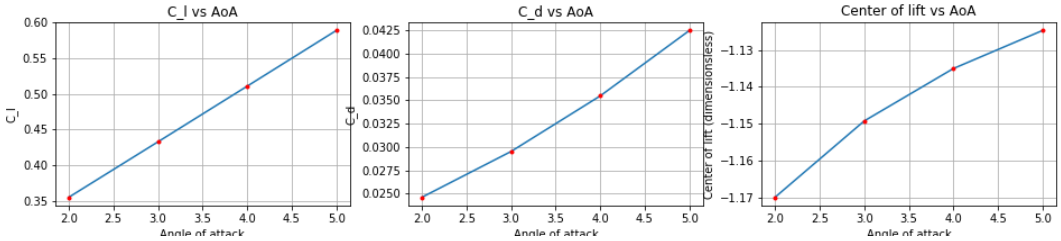

Figure 15: Results from the CFD

Comparing the average slope of the two sets of plots, we saw a promising trend in increased stability. Before, our aircraft's C_L went from -1.25 to -1.18. Now, it went from -1.17 to -1.13 over the same angle range. To summarize, instead of increasing by by .07, it increased by .04 - a better range, but one that still leaves much to be desired.

One observation was that the horizontal tail was enmeshed within the wake of the primary wing (see Figure 16): by placing it on top of the vertical stabilizer, it would be exposed to the freestream and produce an increased stabilizing moment on the aircraft. This is item 3 in the list at the top of this section: changing the position of the horizontal tail.

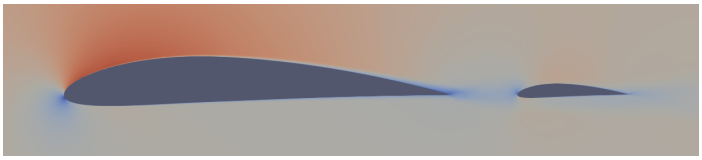

Figure 16: Horizontal tail in the wake of main wing

7.3 Final Report Stability Analysis

As seen in our ESP models and CFD results, we moved the horizontal tail to the top of the vertical stabilizer for our final design. This produced satisfactory stability, with C_L moving further downstream as α increased, seen in Figure 17.

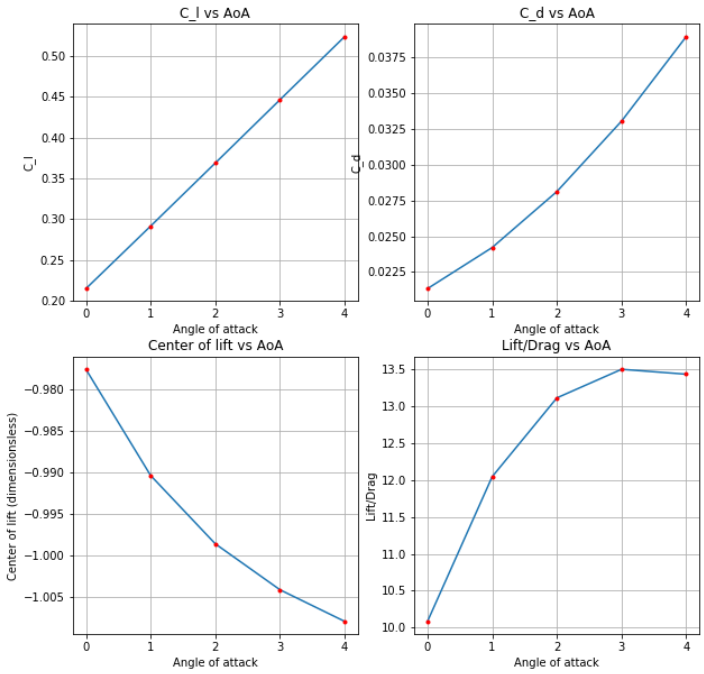

Figure 17: Results from the CFD

8 Final design iteration

This section details the final changes and estimations we made to our aircraft. In order to gain a more complete picture of our aircraft's performance, we accounted for the drag of the horizontal tail (i.e. it is no longer negligible). We assume it has surface area A_h and that the coefficient of drag is close to that of the main wing, as both utilize thick airfoils.

Furthermore, we re-estimate the coefficient of drag of the fuselage using the results from the CFD calculations. We can re-estimate the coefficient of drag at 0 α by looking at $C_d(CFD) = 2.1332e^{-2}$. Then we impose that the total drag is equal for both the CFD and the estimates:

$$C_d(CFD)A_{\text{Ref}} = C_d(\text{estimate Wing})(A_{\text{wing}} + A_{\text{htail}}) + C_d(\text{estimate fuselage})A_{\text{fuselage}} + \frac{\text{Induced Drag}}{0.5\rho V_\infty^2}$$

The left hand side is 0.5333; using the values from our Draft Report, the right hand side is around 4. Therefore, our original estimated drag coefficients are too high - particularly the one for the fuselage - as it was used because it was close to a non-streamlined shape (a bullet), but our fuselage is streamlined. We can now use around 0.003. Using these values the right hand side is very close to 0.5, a much better fit for the CFD. We can repeat our calculations with this new value (keeping all other dimensions and coefficients constant). The results are:

- **Optimal Density:** The final optimal density is 0.3893 kgm^{-3}
- **Optimal Altitude:** By looking at Figure 2, the optimal altitude is approximately 10 Km.

- **Lift:** At this altitude, the Lift Coefficient required for cruise flight is lower than the original value, close to 0.356, meaning we can cruise at a low angle of attack between 1 and 2 degrees.
- **Drag:** The new total drag is: 1923 N. It can be split into:
  - Induced Drag: 961 N
  - Skin Friction: 962 N
- **Power for cruise flight:** The final power estimate is: 269281 W, 269 kW. The VTOL power is the same.
- **Range:** With 2000 Kg of batteries, the range is 2189 Km.
- **Energy:** The energy required for this flight is 4.2 MJ.
- **Solar Effects:** The solar power produced is the same as before, but due to the lower power requirement, it now accounts for 8.9 % of the total power in ideal conditions (using the average solar radiation in Australia and solar panels as described previously). This gives us an enhanced range of 2403 Km when operating in ideal solar conditions.
- **Theoretical Maximum Range:** Using the aforementioned analysis, the theoretical maximum range turns out to be: 9517 km with 10939 Kg of batteries, still an unreasonable amount as $C_L = 1.39$ is too high for this to be possible. The new battery mass vs range graph is available in Figure 18

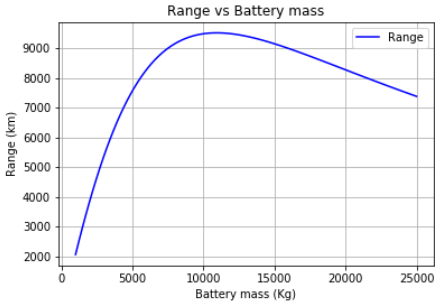

Figure 18: Variation of range wrt battery mass (final)

9 Transition from Hover to Cruise: Take Off

The take off and climbing procedure is as follows:

1. Take off in hover mode using only the wing propellers, similar to a helicopter.
2. Climb slowly to a safe height (around 200m) using only the wing propellers.
3. Once that height is reached and there are no obstacles around (buildings, mountains, bridges...), the front propeller is activated. The aircraft beings to accelerate in the direction normal to the hover, keeping the propellers in hover mode and still climbing, but also accelerating.
4. Once a horizontal speed of around 55 ms^{-1} is reached, the wing propellers start to transition to cruise configuration. At this altitude $\rho \approx 0.9$ so the coefficient of lift is around

$$C_{l_{\text{transition}}} = 0.75$$

which our aircraft can reach at an angle of attack of around 7 to 8 degrees.

5. At around 70 to 80 ms^{-1} (and around 500 m of altitude) the wing propellers reach the cruise configuration, and lift is only achieved from the main wing.

6. The aircraft can now climb to cruise altitude.

9.1 CFD at transition

We performed CFD at the speed where the propellers start positioning themselves in the cruise configuration, 55 ms^{-1}. This is around Mach 0.16. We estimated that the plane will require an angle of attack of 8 degrees to have the necessary lift coefficient. The results are below in Figure 19.

CL:	8.0436e-1	CD:	7.2713e-2		
CFx:	-3.9939e-2	CFy:	-2.9272e-4	CFz:	8.0665e-1
CMx:	-4.6492e-5	CMy:	-8.2332e-1	CMz:	-3.0169e-4

Figure 19: Results from the CFD

Furthermore, in Figure 20 we can observe the pressure distribution on the craft.

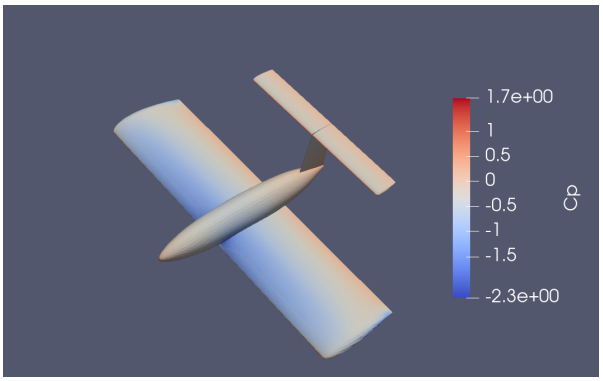

Figure 20: Pressure distribution during transition

In particular we would like to highlight the following aspects:

- The coefficient of lift is 0.8 which is higher than required, meaning we could relax the angle of attack and still have sufficient lift, or, on the contrary, increase it and still have room for a faster ascent.
- The drag coefficient is still low, meaning our lift-to-drag ratio during the climbing phase is still relatively high.

As the angle of attack is relatively high, it is interesting to study the health of the boundary layer as seen in Figure 21b. We can see that the boundary layer is "healthy" because the flow is not separated.

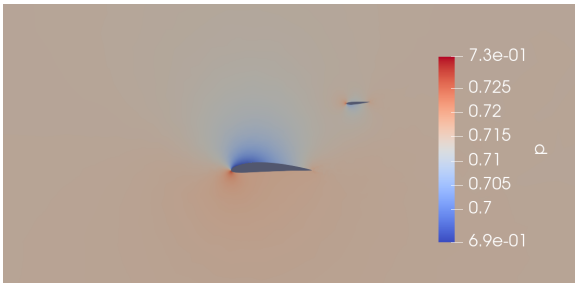

(a) Pressure distribution

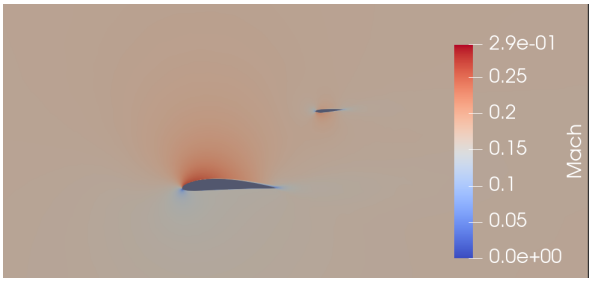

(b) Mach distribution

10 Transition from Cruise to Hover: Landing

1. Start decelerating from cruise speed by reducing the throttle input and controlling the altitude drop from cruise altitude.
2. Once around 50 ms^{-1} and 500m in altitude, the wing propellers start to transition to hover configuration.
3. At around 200 m of altitude, the propellers reach hover configuration and horizontal speed should be close to zero.
4. With all lift coming from the rotated wing propellers, the aircraft can perform a controlled vertical descent to the landing platform.

10.1 Stall performance

We performed CFD analysis at extreme angles of attack - in particular, at 18 degrees - to study the behaviour of the aircraft. We see that the plane still generates significant lift, with a lift coefficient higher than 1, although most of the flow has separated on the inner sections of the wing.

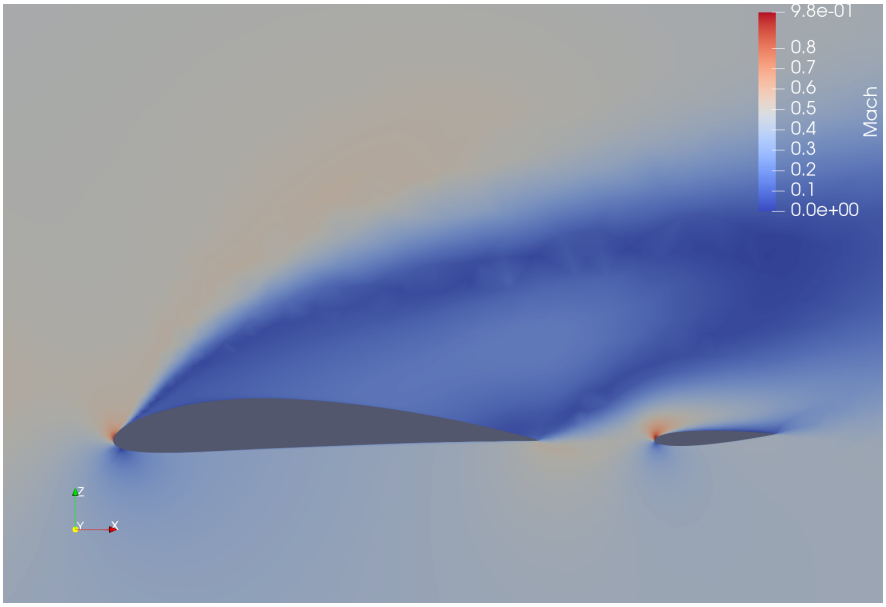

Figure 22: Results from the CFD

11 Conclusion

Our final design is a robust, short-range, fully-electric, VTOL passenger aircraft, with a range of over 2000 Km powered entirely by batteries and solar panels. Its cruise speed of 140 ms^{-1} and cruise altitude of 10 Km creates a high lift-to-drag ratio when coupled with the absence of wake drag and a lower-than-expected coefficient of drag on the fuselage. Additionally, our aircraft's stability and stall performance provide plenty of margin of error should flight conditions be sub-optimal. Overall, this report clearly details the iterative process we took in order to produce this robust aircraft.